LA-UR-16-24788 (Accepted Manuscript)

Strengthening the SDP Relaxation of AC Power Flows with Convex Envelopes, Bound Tightening, and Valid Inequalities

Coffrin, Carleton James
Hijazi, Hassan L
Van Hentenryck, Pascal R

To be published in: IEEE Transactions on Power Systems

DOI to publisher's version: 10.1109/TPWRS.2016.2634586

Permalink to record: http://permalink.lanl.gov/object/view?what=info:lanl-repo/lareport/LA-UR-16-24788

Strengthening the SDP Relaxation of AC Power Flows with Convex Envelopes, Bound Tightening, and Valid Inequalities

Carleton Coffrin, Hassan Hijazi, and Pascal Van Hentenryck

***Abstract*—This work revisits the Semidefine Programming (SDP) relaxation of the AC power flow equations in light of recent results illustrating the benefits of bounds propagation, valid inequalities, and the Convex Quadratic (QC) relaxation. By integrating all of these results into the SDP model a new hybrid relaxation is proposed, which combines the benefits from all of these recent works. This strengthened SDP formulation is evaluated on 71 AC Optimal Power Flow test cases from the NESTA archive and is shown to have an optimality gap of less than 1% on 63 cases. This new hybrid relaxation closes 50% of the open cases considered, leaving only 8 for future investigation.**

***Index Terms*—Optimization Methods, Convex Quadratic Optimization, Semidefine Programming, Optimal Power Flow**

NOMENCLATURE

N	- The set of nodes in the network
E	- The set of *from* edges in the network
$\boldsymbol{i}$	- imaginary number constant
I	- AC current
$S = p + \boldsymbol{i}q$	- AC power
$V = v\angle\theta$	- AC voltage
$Y = g + \boldsymbol{i}b$	- Line admittance
$W = w^R + \boldsymbol{i}w^I$	- Product of two AC voltages
s^u	- Line apparent power thermal limit
θ_{ij}	- Phase angle difference (i.e. $\theta_i - \theta_j$)
ϕ, δ	- Phase angle difference center and offset
$S^d = p^d + \boldsymbol{i}q^d$	- AC power demand
$S^g = p^g + \boldsymbol{i}q^g$	- AC power generation
c_0, c_1, c_2	- Generation cost coefficients
$\Re(\cdot)$	- Real and part of a complex number
$\Im(\cdot)$	- Imaginary part of a complex number
$(\cdot)^*$	- Conjugate of a complex number
$\lvert\cdot\rvert$	- Magnitude of a complex number, l^2-norm
x^l, x^u	- Lower and upper bounds of x
x^σ	- Sum of the bounds (i.e. $x^l + x^u$)
$\breve{x}$	- Convex envelope of x
$\boldsymbol{x}$	- A constant value

C. Coffrin is a staff scientist at Los Alamos National Laboratory, Los Alamos, New Mexico. H. Hijazi is a member of the Optimisation Research Group at DATA61-CSIRO, ACT, Australia; and affiliated with the College of Engineering and Computer Science, The Australian National University, ACT, Australia. Pascal Van Hentenryck is affiliated with the departments of Industrial and Operations Engineering and Computer Science and Engineering at the University of Michigan, Ann Arbor.

A extended technical report version of this work can is available at [1].

I. INTRODUCTION

CONVEX relaxations of the AC power flow equations, such as the Second-Order Cone (SOC) [2], Convex-DistFlow (CDF) [3], Quadratic Convex (QC) [4], Semidefinite Programming (SDP) [5], and Moment-Based [6], [7], [8], [9] relaxations, have attracted significant interest in recent years. Much of the excitement underlying this line of research was ignited when [10] demonstrated that the SDP relaxation provides globally optimal solutions on a variety of AC Optimal Power Flow (AC-OPF) test cases distributed with Matpower [11]. Combining this finding with industrial-strength convex optimization tools (e.g., Gurobi [12], Cplex [13], Mosek [14]) results in a new approach to developing efficient and reliable algorithms for a wide variety of applications in power systems.

It was long thought that the SDP relaxation was the tightest convex relaxation of the power flow equations. However, recent works have demonstrated that realistic test cases can exhibit a non-zero optimality gap with this relaxation [15], [16], [17]. These new test cases also demonstrate that the QC relaxation can be tighter than the SDP relaxation in some cases [18]. This result was further extended in [19] to show that the QC relaxation, when combined with a bound tightening procedure, is stronger than the SDP relaxation in the vast majority of cases. Despite the progress made in [19], at least 16 AC-OPF test cases in NESTA v0.6.0 [16] are considered "open" and still exhibit an optimality gap above 1%.

This work builds on the recent results of [4], [18], [19], [20] to further improve existing convex relaxations in order to close the optimality gap on the remaining open test cases. Its main contributions can be summarized as follows. The paper

1) develops stronger power flow relaxations dominating the established SDP [10] and QC [4] methods;
2) presents computational results demonstrating that the optimality gap on many of the open test cases can be reduced to less than 1%, using a combination of the methods developed herein.

The computational study is conducted on 71 AC Optimal Power Flow test cases from NESTA v0.6.0, which feature realistic side-constraints and incorporate bus shunts, line charging, and transformers.

The rest of the paper is organized as follows. Section II reviews the formulation of the AC-OPF problem from first principles and presents the key operational side constraints for AC network operations. Section III derives the established SDP and QC relaxations. Section IV presents three orthogonal

and compositional methods for tightening convex relaxations and applies those to the AC power flow constraints. Section V reports the benefits of the various tightening methods on AC-OPF test cases, and Section VI concludes the paper.

II. AC Optimal Power Flow

This section reviews the foundations of AC power network optimization and combines those foundations to derive the seminal AC-OPF problem. Additionally, this section also introduces the notations used throughout the paper. In the following equations, bold face indicates constant values and capital letters indicate complex numbers.

Power networks are comprised of many different types of components, such as generators, loads, buses, and lines. Considered at a system level, the set of buses N and the set of lines E can be interpreted as a graph (N, E), where nodes represent buses and edges correspond to lines. It is important to define E as an undirected collection of edges. However, each line $(i, j) \in E$ is assigned a *from* side (i, j) and a *to* side (j, i) arbitrarily, so that line losses are captured as power flows from one side to another. Typically, a reference bus $r \in N$ is also designated, to allow easy comparison of solutions and to remove symmetric solutions.

The flow of power in the network is defined by the AC power flow equations. These equations link the complex quantities of current I, voltage V, power S, and admittance Y, via the physical properties of Kirchhoff's Current Law (KCL), Ohm's Law, and the definition of AC power. Combining these three properties yields the well known AC Power Flow equations,

$$S_i^g - \boldsymbol{S}_i^d = \sum_{(i,j)\in E} S_{ij} + \sum_{(j,i)\in E} S_{ij} \quad \forall i \in N \tag{1a}$$

$$S_{ij} = \boldsymbol{Y}_{ij}^* V_i V_i^* - \boldsymbol{Y}_{ij}^* V_i V_j^* \quad (i,j),(j,i) \in E \tag{1b}$$

A detailed derivation of these equations can be found in [18]. It is important to note that, for each bus $i \in N$, $\sum$ over $(i, j) \in E$ collects the power flow oriented in the *from* direction and $\sum$ over $(j, i) \in E$ collects the power flow oriented in the *to* direction.

The non-convex nonlinear equations (1a)–(1b) form the core building block of many power network optimization applications. However, each particular application augments these equations with its own particular side constraints. The most common power network optimization side constraints include,

$$\Re(\boldsymbol{S}_i^{\boldsymbol{gl}}) \leqslant \Re(S_i^g) \leqslant \Re(\boldsymbol{S}_i^{\boldsymbol{gu}}) \quad \forall i \in N \tag{2}$$

$$\Im(\boldsymbol{S}_i^{\boldsymbol{gl}}) \leqslant \Im(S_i^g) \leqslant \Im(\boldsymbol{S}_i^{\boldsymbol{gu}}) \quad \forall i \in N \tag{3}$$

$$(\boldsymbol{v}_i^{\boldsymbol{l}})^2 \leqslant |V_i|^2 \leqslant (\boldsymbol{v}_i^{\boldsymbol{u}})^2 \quad \forall i \in N \tag{4}$$

$$|S_{ij}| \leqslant \boldsymbol{s}_{ij}^{\boldsymbol{u}} \quad \forall (i,j),(j,i) \in E \tag{5}$$

$$\tan(\boldsymbol{\theta}_{ij}^{\boldsymbol{l}})\Re(V_i V_j^*) \leqslant \Im(V_i V_j^*) \leqslant \tan(\boldsymbol{\theta}_{ij}^{\boldsymbol{u}})\Re(V_i V_j^*) \ \forall (i,j) \in E \tag{6}$$

Constraints (2)–(3) set limits on the real and reactive generator capabilities, respectively. Constraints (4) limit the magnitudes of bus voltages. Constraints (5) limit the power flow on the lines and constraints (6) limit the difference of the phase angles (i.e. θ_i, θ_j) between the lines' buses. A detailed derivation and further explanation of these operational side constraints can be found in [18].

Typically, the Phase Angle Difference (PAD) constraints (6) have been considered with symmetrical bounds on θ_{ij}, namely,

$$0 \leqslant \boldsymbol{\theta}_{ij}^{\boldsymbol{u}} \leqslant \frac{\boldsymbol{\pi}}{2} \quad \forall (i,j) \in E \tag{7a}$$

$$\boldsymbol{\theta}_{ij}^{\boldsymbol{l}} = -\boldsymbol{\theta}_{ij}^{\boldsymbol{u}} \quad \forall (i,j) \in E \tag{7b}$$

A key insight of [19], which is also used here, is to consider generalized PAD constraints, which are asymmetrical, i.e.,

$$-\frac{\boldsymbol{\pi}}{2} \leqslant \boldsymbol{\theta}_{ij}^{\boldsymbol{l}} \leqslant \boldsymbol{\theta}_{ij}^{\boldsymbol{u}} \leqslant \frac{\boldsymbol{\pi}}{2} \quad \forall (i,j) \in E \tag{8}$$

The usefulness of these asymmetrical PAD constraints will be apparent later in the paper.

The last component in formulating an optimization problem is an objective function. In the power network literature two objective functions are typically considered, line loss minimization and generator fuel cost minimization, i.e.,

$$\text{minimize:} \ \sum_{i\in N} \boldsymbol{c}_{2i}(\Re(S_i^g))^2 + \boldsymbol{c}_{1i}\Re(S_i^g) + \boldsymbol{c}_{0i} \tag{9}$$

Note that line loss minimization is a special case of (9) where $\boldsymbol{c}_{2i} = 0, \boldsymbol{c}_{1i} = 1, \boldsymbol{c}_{0i} = 0 \quad (\forall i \in N)$ [21]. Hence, this work focuses exclusively on objective (9) without any loss of generality.

The AC Optimal Power Flow Problem: Model 1 combines the AC power flow equations, the side constraints, and the objective function, to produce the seminal AC-OPF problem [22]. This formulation utilizes a voltage product factorization (i.e. $V_i V_j^* = W_{ij} \quad \forall (i,j) \in E$), a complete derivation of this formulation can be found in [18]. Model 1 is a non-convex nonlinear optimization problem, which is NP-Hard [23], [24]. In practice, the AC-OPF problem is solved with numerical methods [25], [26], which are not guaranteed to converge to a feasible point and only provide locally optimal solutions when they do converge.

A key message throughout this work and the related works [18], [19] is that the bounds on the decision variables are a critical consideration in the AC-OPF problem. Hence, the variable bounds are explicitly specified in Model 1. Noting that bounds on the variables V, W, S are most often omitted from power network datasets, we present valid bounds here. Suitable bounds for V and S can be deduced from the bus voltage and thermal limit constraints as follows,

$$\boldsymbol{V}_i^{\boldsymbol{u}} = \boldsymbol{v}_i^{\boldsymbol{u}} + \boldsymbol{i}\boldsymbol{v}_i^{\boldsymbol{u}}, \boldsymbol{V}_{ij}^{\boldsymbol{l}} = -(\boldsymbol{v}_i^{\boldsymbol{u}} + \boldsymbol{i}\boldsymbol{v}_i^{\boldsymbol{u}}) \quad \forall i \in N$$
$$\boldsymbol{S}_{ij}^{\boldsymbol{u}} = \boldsymbol{s}_{ij}^{\boldsymbol{u}} + \boldsymbol{i}\boldsymbol{s}_{ij}^{\boldsymbol{u}}, \boldsymbol{S}_{ij}^{\boldsymbol{l}} = -(\boldsymbol{s}_{ij}^{\boldsymbol{u}} + \boldsymbol{i}\boldsymbol{s}_{ij}^{\boldsymbol{u}}) \quad \forall (i,j) \in E$$

A derivation of these bounds can be found in [27]. The bounds on the diagonal values of W are,

$$\boldsymbol{W}_{ii}^{\boldsymbol{u}} = (\boldsymbol{v}_i^{\boldsymbol{u}})^2 + \boldsymbol{i}0, \boldsymbol{W}_{ii}^{\boldsymbol{l}} = (\boldsymbol{v}_i^{\boldsymbol{l}})^2 + \boldsymbol{i}0 \quad \forall i \in N$$

Model 1 The AC Optimal Power Flow Problem (AC-OPF).

variables:

$S_i^g \in (\boldsymbol{S_i^{gl}}, \boldsymbol{S_i^{gu}}) \ \ \forall i \in N$

$V_i \in (\boldsymbol{V_i^l}, \boldsymbol{V_i^u}) \ \ \forall i \in N$

$W_{ij} \in (\boldsymbol{W_{ij}^l}, \boldsymbol{W_{ij}^u}) \ \ \forall i \in N, \forall j \in N$

$S_{ij} \in (\boldsymbol{S_{ij}^l}, \boldsymbol{S_{ij}^u}) \ \ \forall (i,j), (j,i) \in E$

minimize:

$$\sum_{i \in N} \boldsymbol{c}_{2i}(\Re(S_i^g))^2 + \boldsymbol{c}_{1i}\Re(S_i^g) + \boldsymbol{c}_{0i} \tag{10a}$$

subject to:

$$\angle V_{\boldsymbol{r}} = 0 \tag{10b}$$

$$W_{ij} = V_i V_j^* \ \ \forall (i,j) \in E \tag{10c}$$

$$S_i^g - \boldsymbol{S}_i^d = \sum_{(i,j) \in E} S_{ij} + \sum_{(j,i) \in E} S_{ij} \ \ \forall i \in N \tag{10d}$$

$$S_{ij} = \boldsymbol{Y}_{ij}^* W_{ii} - \boldsymbol{Y}_{ij}^* W_{ij} \ \ \forall (i,j) \in E \tag{10e}$$

$$S_{ji} = \boldsymbol{Y}_{ij}^* W_{jj} - \boldsymbol{Y}_{ij}^* W_{ij}^* \ \ \forall (i,j) \in E \tag{10f}$$

$$|S_{ij}| \leqslant (\boldsymbol{s_{ij}^u}) \ \ \forall (i,j), (j,i) \in E \tag{10g}$$

$$\tan(\boldsymbol{\theta_{ij}^l})\Re(W_{ij}) \leqslant \Im(W_{ij}) \leqslant \tan(\boldsymbol{\theta_{ij}^u})\Re(W_{ij}) \ \ \forall (i,j) \in E \tag{10h}$$

which captures the bus voltage limit constraints (4). Lastly, the bounds on the off diagonal elements, i.e. $(i,j) \in E$, are,

$$\boldsymbol{W_{ij}^u} = \begin{cases} \boldsymbol{v_i^u v_j^u} \cos(\boldsymbol{\theta_{ij}^u}) + \boldsymbol{i v_i^l v_j^l} \sin(\boldsymbol{\theta_{ij}^u}) & \text{if } \boldsymbol{\theta_{ij}^l}, \boldsymbol{\theta_{ij}^u} \leqslant 0 \\ \boldsymbol{v_i^u v_j^u} \cos(\boldsymbol{\theta_{ij}^l}) + \boldsymbol{i v_i^u v_j^u} \sin(\boldsymbol{\theta_{ij}^u}) & \text{if } \boldsymbol{\theta_{ij}^l}, \boldsymbol{\theta_{ij}^u} \geqslant 0 \\ \boldsymbol{v_i^u v_j^u} + \boldsymbol{i v_i^u v_j^u} \sin(\boldsymbol{\theta_{ij}^u}) & \text{if } \boldsymbol{\theta_{ij}^l} < 0, \boldsymbol{\theta_{ij}^u} > 0 \end{cases}$$

$$\boldsymbol{W_{ij}^l} = \begin{cases} \boldsymbol{v_i^l v_j^l} \cos(\boldsymbol{\theta_{ij}^l}) + \boldsymbol{i v_i^u v_j^u} \sin(\boldsymbol{\theta_{ij}^l}) & \text{if } \boldsymbol{\theta_{ij}^l}, \boldsymbol{\theta_{ij}^u} \leqslant 0 \\ \boldsymbol{v_i^l v_j^l} \cos(\boldsymbol{\theta_{ij}^u}) + \boldsymbol{i v_i^l v_j^l} \sin(\boldsymbol{\theta_{ij}^l}) & \text{if } \boldsymbol{\theta_{ij}^l}, \boldsymbol{\theta_{ij}^u} \geqslant 0 \\ \min(\boldsymbol{v_i^l v_j^l} \cos(\boldsymbol{\theta_{ij}^l}), \boldsymbol{v_i^l v_j^l} \cos(\boldsymbol{\theta_{ij}^u})) & \\ \qquad + \boldsymbol{i v_i^u v_j^u} \sin(\boldsymbol{\theta_{ij}^l}) & \text{if } \boldsymbol{\theta_{ij}^l} < 0, \boldsymbol{\theta_{ij}^u} > 0 \end{cases}$$

A derivation of these bounds can be found in [1]. Note that, all of the decision variables in Model 1 have well defined bounds parameterized by $\boldsymbol{v_i^l}, \boldsymbol{v_i^u}, \boldsymbol{s_{ij}^u}, \boldsymbol{\theta_{ij}^l}, \boldsymbol{\theta_{ij}^u}$, which are readily available in power network datasets [16].

Model Extensions: In the interest of clarity, the simplest version of the AC power flow equations is most often used to present power network optimization models. However, transmission system test cases include additional parameters such as line charging, transformers, and bus shunts, which make the AC power flow equations significantly more complicated. In this work, all of the results focus exclusively on the voltage product constraint (10c). As a consequence, the results can be seamlessly extended to these more general cases by modifying the constant parameters in constraints (10d)–(10f). Real-world deployment of AC-OPF methods require even more extensions, discussed at length in [28], [29]. For similar reasons, it is likely that the results presented here will also extend to those real-world variants.

Model 2 The SDP Relaxation (AC-OPF-SDP).

variables: $S_i^g (\forall i \in N)$, $W_{ij} (\forall i \in N, \forall j \in N)$, $S_{ij} (\forall (i,j), (j,i) \in E)$

minimize: (10a)

subject to: (10d)–(10h)

$$W \succeq 0 \tag{12a}$$

III. Convex Relaxations of Optimal Power Flow

Since the AC-OPF problem (i.e. Model 1) is non-convex and NP-Hard [23], [24], numerical methods can provide limited guarantees for determining feasibility and global optimally of these problems. In contrast, a convex relaxation of AC-OPF provides a computationally efficient method to:

1) produce lower bounds on the objective function;
2) prove infeasibility of a particular instance;
3) produce a solution that is feasible in the original non-convex problem, thus solving the AC-OPF problem and guaranteeing that the solution is globally optimal [10].

The ability to provide objective bounds is particularly important for bounding the quality of solutions produced by locally optimal methods and is also an invaluable tool for solving the numerous mixed-integer nonlinear optimization problems that arise in power system applications [30]. Motivated by these advantages, a variety of convex relaxations have been developed for the AC-OPF including the, SOC [2], Convex-DistFlow [3], [31], QC [4], and SDP [5] relaxations, to name a few.

It has been established that the SOC and Convex-DistFlow relaxations are equivalent [32], [31] and that the SOC relaxation is dominated by the SDP and QC relaxations [33], [18]. In light of these results, this work focuses on the SDP and QC relaxations and reviews how they are derived from Model 1. The key distinguishing feature of each relaxation is the convexification of (10c), which are the exclusive source of non-convexity in Model 1.

The Semidefinite Programming (SDP) Relaxation: utilizes the insight that the W variables can be interpreted as a matrix defined by $V(V^*)^T$ ensuring that W is positive semidefinite (denoted by $W \succeq 0$) and has rank 1 [5], [10], [33]. These conditions are sufficient to enforce the constraints (10c) [34], namely,

$$W_{ij} = V_i V_j^* \ \ \forall i,j \in N \ \ \Leftrightarrow \ \ W \succeq 0 \ \ \wedge \ \ \text{rank}(W) = 1$$

A convex SDP relaxation simply ignores the non-convex rank constraint [35], [34] resulting in Model 2.

The Quadratic Convex (QC) Relaxation: proposed in [4] is inspired by an arithmetic analysis of (10c) in polar coordinates (i.e., $V_i = v_i \angle \theta_i \ \ \forall i \in N$). The polar voltage variables v, θ can then be connected to the W variables using the following, well known [36], [37], [38], [39], equations:

$$W_{ii} = v_i^2 \ \ i \in N \tag{13a}$$

$$\Re(W_{ij}) = v_i v_j \cos(\theta_{ij}) \ \ \forall (i,j) \in E \tag{13b}$$

$$\Im(W_{ij}) = v_i v_j \sin(\theta_{ij}) \ \ \forall (i,j) \in E \tag{13c}$$

Model 3 The QC Relaxation (AC-OPF-QC).

variables: $S_i^g(\forall i \in N),\ W_{ij}(\forall (i,j) \in E),\ W_{ii}(\forall i \in N),$
$v_i \angle \theta_i(\forall i \in N),\ S_{ij}(\forall (i,j),(j,i) \in E)$
minimize: (10a)
subject to: (10d)–(10h)

$$|W_{ij}|^2 \leqslant W_{ii} W_{jj} \quad \forall (i,j) \in E \tag{14a}$$
$$\theta_{\boldsymbol{r}} = 0 \tag{14b}$$
$$W_{ii} = \langle v_i^2 \rangle^T \quad i \in N \tag{14c}$$
$$\Re(W_{ij}) = \langle \langle v_i v_j \rangle^M \langle \cos(\theta_{ij}) \rangle^C \rangle^M \quad \forall (i,j) \in E \tag{14d}$$
$$\Im(W_{ij}) = \langle \langle v_i v_j \rangle^M \langle \sin(\theta_{ij}) \rangle^S \rangle^M \quad \forall (i,j) \in E \tag{14e}$$

The QC model relaxes these non-convex equations by composing convex envelopes of the non-convex nonlinear subexpressions. The process of developing these convex envelopes utilizes the bounds on v_i, v_j, θ_{ij} to define tight convex regions. For example, the convex envelopes for the square and product of variables are well-known [40], i.e.,

$$\langle x^2 \rangle^T \equiv \begin{cases} \breve{x} \geqslant x^2 \\ \breve{x} \leqslant (\boldsymbol{x^u} + \boldsymbol{x^l})x - \boldsymbol{x^u x^l} \end{cases} \tag{T-CONV}$$

$$\langle xy \rangle^M \equiv \begin{cases} \widetilde{xy} \geqslant \boldsymbol{x^l} y + \boldsymbol{y^l} x - \boldsymbol{x^l y^l} \\ \widetilde{xy} \geqslant \boldsymbol{x^u} y + \boldsymbol{y^u} x - \boldsymbol{x^u y^u} \\ \widetilde{xy} \leqslant \boldsymbol{x^l} y + \boldsymbol{y^u} x - \boldsymbol{x^l y^u} \\ \widetilde{xy} \leqslant \boldsymbol{x^u} y + \boldsymbol{y^l} x - \boldsymbol{x^u y^l} \end{cases} \tag{M-CONV}$$

Observe how these envelopes are parameterized by the variable bounds (i.e. $\boldsymbol{x^l}, \boldsymbol{x^u}, \boldsymbol{y^l}, \boldsymbol{y^u}$).

The original QC formulation [4] proposed convex envelopes for sine and cosine functions with symmetrical PAD constraints. The envelopes developed below are a slight generalization of those formulations, which support asymmetrical PAD constraints. Under the assumption that the phase angle difference bound is within $-\boldsymbol{\pi}/2 \leqslant \boldsymbol{\theta^l_{ij}} \leqslant \boldsymbol{\theta^u_{ij}} \leqslant \boldsymbol{\pi}/2$, convex envelopes for sine (S-CONV) and cosine (C-CONV) are given by,

$$\langle \sin(x) \rangle^S \equiv \begin{cases} \widetilde{sx} \leqslant \cos\left(\frac{\boldsymbol{x^m}}{2}\right)\left(x - \frac{\boldsymbol{x^m}}{2}\right) + \sin\left(\frac{\boldsymbol{x^m}}{2}\right) \\ \widetilde{sx} \geqslant \cos\left(\frac{\boldsymbol{x^m}}{2}\right)\left(x + \frac{\boldsymbol{x^m}}{2}\right) - \sin\left(\frac{\boldsymbol{x^m}}{2}\right) \\ \widetilde{sx} \geqslant \frac{\sin(\boldsymbol{x^l}) - \sin(\boldsymbol{x^u})}{(\boldsymbol{x^l} - \boldsymbol{x^u})}(x - \boldsymbol{x^l}) + \sin(\boldsymbol{x^l}) \text{ if } \boldsymbol{x^l} \geqslant 0 \\ \widetilde{sx} \leqslant \frac{\sin(\boldsymbol{x^l}) - \sin(\boldsymbol{x^u})}{(\boldsymbol{x^l} - \boldsymbol{x^u})}(x - \boldsymbol{x^l}) + \sin(\boldsymbol{x^l}) \text{ if } \boldsymbol{x^u} \leqslant 0 \end{cases}$$

$$\langle \cos(x) \rangle^C \equiv \begin{cases} \widetilde{cx} \leqslant 1 - \frac{1 - \cos(\boldsymbol{x^m})}{(\boldsymbol{x^m})^2} x^2 \\ \widetilde{cx} \geqslant \frac{\cos(\boldsymbol{x^l}) - \cos(\boldsymbol{x^u})}{(\boldsymbol{x^l} - \boldsymbol{x^u})}(x - \boldsymbol{x^l}) + \cos(\boldsymbol{x^l}) \end{cases}$$

where $\boldsymbol{x^m} = \max(|\boldsymbol{x^l}|, |\boldsymbol{x^u}|)$.

Model 4 The SDP & QC Relaxation (AC-OPF-SDP+QC).

variables: $S_i^g(\forall i \in N),\ W_{ij}(\forall i \in N, \forall j \in N),$
$v_i \angle \theta_i(\forall i \in N),\ S_{ij}(\forall (i,j),(j,i) \in E)$
minimize: (10a)
subject to: (10d)–(10h), (12a), (14b)–(14e)

A convex relaxation of the equations (13a)–(13c) can then be developed by composing the convex envelopes for square, sine, cosine, and the product of two variables, as follows,

$$W_{ii} = \langle v_i^2 \rangle^T \quad i \in N \tag{15a}$$
$$\Re(W_{ij}) = \langle \langle v_i v_j \rangle^M \langle \cos(\theta_{ij}) \rangle^C \rangle^M \quad \forall (i,j) \in E \tag{15b}$$
$$\Im(W_{ij}) = \langle \langle v_i v_j \rangle^M \langle \sin(\theta_{ij}) \rangle^S \rangle^M \quad \forall (i,j) \in E \tag{15c}$$

Lastly, [4] proposes to strengthen the QC relaxation with the second-order cone constraint from the SOC relaxation [2], i.e.,

$$|W_{ij}|^2 \leqslant W_{ii} W_{jj} \tag{16}$$

Although it may appear non-convex, (16) is in fact a rotated second-order cone constraint, which is readily supported by industrial convex optimization tools.

The complete QC relaxation is presented in Model 3. A key observation about the QC relaxation is that the convex envelopes are determined by the variable bounds; the tighter the bounds are, the stronger the relaxation becomes [18], [19].

IV. Strengthening Convex Relaxations

It has been established that the SDP and QC relaxations have different strengths and weaknesses and one does not dominate the other [18], [19]. In this work, we develop a hybrid relaxation, which dominates both formulations. This is accomplished by considering three orthogonal and compositional approaches to strengthening relaxations:

1) Model Intersection (e.g. [41], [42])
2) Valid Inequalities (e.g. [17], [43])
3) Bound Tightening (e.g. [19], [44])

The rest of this section explains how each of these ideas is utilized to strengthen the SDP relaxation.

A. Model Intersection

Given that the SDP and QC relaxations have different strengths and weaknesses [18], a natural and straightforward way to obtain a stronger relaxation is to combine them, yielding a feasible set that is the intersection of both relaxations. Model 4 presents such a model.

The second order cone constraint in the QC (14a) is redundant in Model 4 and can be omitted. The reasoning is that the positive semidefinite constraint (12a) ensures that every submatrix of W is positive semidefinite [45]. This includes the following 2-by-2 sub-matrices for each line,

$$\begin{bmatrix} W_{ii} & W_{ij} \\ W_{ij}^* & W_{jj} \end{bmatrix} \succeq 0 \quad \forall (i,j) \in E$$

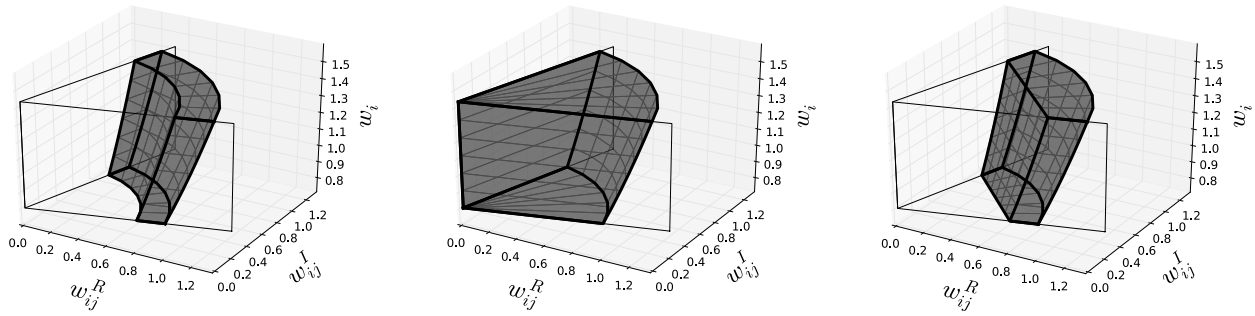

(a) Non-Convex Set (b) Convex Relaxation (c) Strengthened Convex Relaxation

Fig. 1: The Implications of the Valid Inequalities, such as Lifted Nonlinear Cuts (LNCs), on the Convexification of (20).

Model 5 The Non-Convex Voltage Feasibility Set ($\forall (i,j) \in E$).

$$\begin{aligned}
\textbf{variables: } & W_{ii} = w_i, W_{jj} = w_j, W_{ij} = w_{ij}^R + \boldsymbol{i} w_{ij}^I \\
\textbf{subject to: } & (\boldsymbol{v}_i^{\boldsymbol{l}})^2 \leqslant w_i \leqslant (\boldsymbol{v}_i^{\boldsymbol{u}})^2 && \text{(21a)} \\
& (\boldsymbol{v}_j^{\boldsymbol{l}})^2 \leqslant w_j \leqslant (\boldsymbol{v}_j^{\boldsymbol{u}})^2 && \text{(21b)} \\
& \tan(\boldsymbol{\theta}_{ij}^{\boldsymbol{l}}) w_{ij}^R \leqslant w_{ij}^I \leqslant \tan(\boldsymbol{\theta}_{ij}^{\boldsymbol{u}}) w_{ij}^R && \text{(21c)} \\
& (w_{ij}^R)^2 + (w_{ij}^I)^2 = w_i w_j && \text{(21d)}
\end{aligned}$$

Applying the determinant characterization for positive semidefinite matrices yields

$$\begin{aligned}
& 0 \leqslant W_{ii} W_{jj} - W_{ij} W_{ij}^* \;\; \forall (i,j) \in E \\
& |W_{ij}|^2 \leqslant W_{ii} W_{jj} \;\; \forall (i,j) \in E
\end{aligned}$$

which is equivalent to (14a).

B. Valid Inequalities

It was recently demonstrated that valid inequalities can be used to strengthen the SDP and SOC relaxations [17], [43]. To better understand how relaxations benefit from valid inequalities, let us consider a specific example in detail.

1) The Benefits of Valid Inequalities: The fundamental source of nonconvexity in (AC-OPF) is,

$$W_{ij} = V_i V_j^* \;\; \forall (i,j) \in E. \tag{19}$$

Applying the absolute square to this constraint yields,

$$|W_{ij}|^2 = W_{ii} W_{jj} \;\; \forall (i,j) \in E \tag{20}$$

which is a valid and redundant constraint in any AC power flow model. Incidentally, (20) is a stronger nonconvex version of (16), which is a key component of all nonlinear power flow relaxations.

Now let us consider the set of feasible points defined by (20), the voltage magnitude bounds (4), and the PAD constraints (6). Model 5 presents such a model, with the complex variables expanded into their real number representation and the voltage bounds modeled explicitly as constraints. Model 5 is defined over $(w_{ij}^R, w_{ij}^I, w_i, w_j) \in \mathbb{R}^4$, however, we observe that the nonlinear equation (21d) can be used to eliminate one of the variables, reducing the variable space to $\mathbb{R}^3$. We use $((w_{ij}^R)^2 + (w_{ij}^I)^2)/w_i = w_j$ to eliminate the w_j variable and focus on the $(w_{ij}^R, w_{ij}^I, w_i) \in \mathbb{R}^3$ space.

Figure 1 presents the feasible set of Model 5 in the $(w_{ij}^R, w_{ij}^I, w_i)$ space with the following realistic parameters:

$$\begin{aligned}
& \boldsymbol{v}_i^{\boldsymbol{l}} = 0.9, \;\; \boldsymbol{v}_i^{\boldsymbol{u}} = 1.2, \;\; \boldsymbol{v}_j^{\boldsymbol{l}} = 0.8, \;\; \boldsymbol{v}_j^{\boldsymbol{u}} = 1.0, \\
& \boldsymbol{\theta}_{ij}^{\boldsymbol{l}} = \boldsymbol{\pi}/12, \;\; \boldsymbol{\theta}_{ij}^{\boldsymbol{u}} = 5\boldsymbol{\pi}/12
\end{aligned}$$

To illustrate the value of valid inequalities in the convexification of (20), Figure 1 highlights three variants of Model 5. Figure 1a presents the true nonconvex set of Model 5. Figure 1b illustrates a standard convex relaxation of Model 5 (i.e., (16)), and Figure 1c shows the tightest convex relaxation of Model 5, which is achieved through valid inequalities. The significant reduction in the feasible set in Figure 1c (when compared to Figure 1b) results in a tighter relaxation and smaller optimality gaps.

2) The Lifted Nonlinear Cuts (LNCs): In this work, we utilize two valid inequalities for Model 5 called the Lifted Nonlinear Cuts (LNCs), which were independently proposed in both [1] and [46]. Let us define the following constants based on the variable bounds:

$$\boldsymbol{v}_i^{\boldsymbol{\sigma}} = \boldsymbol{v}_i^{\boldsymbol{l}} + \boldsymbol{v}_i^{\boldsymbol{u}} \;\; \forall i \in N \tag{24a}$$

$$\boldsymbol{\phi}_{ij} = (\boldsymbol{\theta}_{ij}^{\boldsymbol{u}} + \boldsymbol{\theta}_{ij}^{\boldsymbol{l}})/2 \;\; \forall (i,j) \in E \tag{24b}$$

$$\boldsymbol{\delta}_{ij} = (\boldsymbol{\theta}_{ij}^{\boldsymbol{u}} - \boldsymbol{\theta}_{ij}^{\boldsymbol{l}})/2 \;\; \forall (i,j) \in E. \tag{24c}$$

The LNCs are given by (23a)-(23b), and are linear in the $w_i, w_j, w_{ij}^R, w_{ij}^I$ space. A proof of the validity of these cuts and the inspiration for the name "lifted nonlinear cuts" can be found in [1].

A variety of valid inequalities have been proposed for (AC-OPF) [17], [43], [1], [47], [46]. We chose to use the LNCs since we have shown in [1] that LNCs are guaranteed to be stronger than the cuts proposed in [17], [47]. Additionally, the LNCs produce the convex hull pictured in Figure 1c and it is suggested in [46] that (16) strengthened with LNCs defines the convex hull of Model 5.

C. Bound Tightening

It is observed in [19] that both the SDP and QC models benefit significantly from tightening the bounds on variables v_i and θ_{ij}. Since this also holds for the LNCs, we utilize the

$$\boldsymbol{v}_i^{\boldsymbol{\sigma}}\boldsymbol{v}_j^{\boldsymbol{\sigma}}(w_{ij}^R\cos(\boldsymbol{\phi}_{ij})+w_{ij}^I\sin(\boldsymbol{\phi}_{ij}))-\boldsymbol{v}_j^{\boldsymbol{u}}\cos(\boldsymbol{\delta}_{ij})\boldsymbol{v}_j^{\boldsymbol{\sigma}}w_i-\boldsymbol{v}_i^{\boldsymbol{u}}\cos(\boldsymbol{\delta}_{ij})\boldsymbol{v}_i^{\boldsymbol{\sigma}}w_j\geqslant\boldsymbol{v}_i^{\boldsymbol{u}}\boldsymbol{v}_j^{\boldsymbol{u}}\cos(\boldsymbol{\delta}_{ij})(\boldsymbol{v}_i^{\boldsymbol{l}}\boldsymbol{v}_j^{\boldsymbol{l}}-\boldsymbol{v}_i^{\boldsymbol{u}}\boldsymbol{v}_j^{\boldsymbol{u}})\ \forall(i,j)\in E \quad (23a)$$

$$\boldsymbol{v}_i^{\boldsymbol{\sigma}}\boldsymbol{v}_j^{\boldsymbol{\sigma}}(w_{ij}^R\cos(\boldsymbol{\phi}_{ij})+w_{ij}^I\sin(\boldsymbol{\phi}_{ij}))-\boldsymbol{v}_j^{\boldsymbol{l}}\cos(\boldsymbol{\delta}_{ij})\boldsymbol{v}_j^{\boldsymbol{\sigma}}w_i-\boldsymbol{v}_i^{\boldsymbol{l}}\cos(\boldsymbol{\delta}_{ij})\boldsymbol{v}_i^{\boldsymbol{\sigma}}w_j\geqslant\boldsymbol{v}_i^{\boldsymbol{l}}\boldsymbol{v}_j^{\boldsymbol{l}}\cos(\boldsymbol{\delta}_{ij})(\boldsymbol{v}_i^{\boldsymbol{u}}\boldsymbol{v}_j^{\boldsymbol{u}}-\boldsymbol{v}_i^{\boldsymbol{l}}\boldsymbol{v}_j^{\boldsymbol{l}})\ \ \forall(i,j)\in E \quad (23b)$$

Algorithm 1 Bound Tightening for v and θ Variables.

repeat
  $\boldsymbol{v^{l0}}, \boldsymbol{v^{u0}}, \boldsymbol{\theta^{l0}}, \boldsymbol{\theta^{u0}} := \boldsymbol{v^l}, \boldsymbol{v^u}, \boldsymbol{\theta^l}, \boldsymbol{\theta^u}$;
  let $\Omega :=$ Model 3 **given** $\boldsymbol{v^l}, \boldsymbol{v^u}, \boldsymbol{\theta^l}, \boldsymbol{\theta^u}$;
  for all $i \in N$
    $\boldsymbol{v_i^l} := \min v_i \in \Omega$;
    $\boldsymbol{v_i^u} := \max v_i \in \Omega$;
  for all $(i,j) \in E$
    $\boldsymbol{\theta_{ij}^l} := \min \theta_{ij} \in \Omega$;
    $\boldsymbol{\theta_{ij}^u} := \max \theta_{ij} \in \Omega$;
until $\boldsymbol{v^{l0}}, \boldsymbol{v^{u0}}, \boldsymbol{\theta^{l0}}, \boldsymbol{\theta^{u0}} = \boldsymbol{v^l}, \boldsymbol{v^u}, \boldsymbol{\theta^l}, \boldsymbol{\theta^u}$;
return $\boldsymbol{v^l}, \boldsymbol{v^u}, \boldsymbol{\theta^l}, \boldsymbol{\theta^u}$;

minimal network consistency algorithm proposed in [19] to strengthen all of the relaxations considered here.

The minimal network consistency algorithm is presented in Algorithm 1 works as follows. First, a QC relaxation of the AC-OPF problem is constructed (i.e. Ω). Then, the objective function is modified to compute the largest or the smallest value of v_i and θ_{ij}. This process is repeated for all of the buses and lines in the network, resulting in a total of $2|N| + 2|E|$ convex quadratic optimization problems. Upon completing all of these optimizations, the variable bounds have been strengthened and, if any bound has decreased, a tighter QC relaxation can be constructed. After reconstructing a updated QC relaxation, it is possible that the bounds can be tightened further. Hence, this processes is repeated until a fixed-point is reached (i.e. none of the bounds change). A detailed description and an in-depth analysis of this bound-tightening procedure can be found in [19].

Note that all of the optimization problems in each round of Algorithm 1 are independent and can be computed in parallel. Hence, the this algorithm is highly parallelizable and the total runtime is roughly the time of one network solve multiplied by the number of rounds before reaching the fix-point (the number of rounds required was estimated to be around 5–10 in [19]). Clearly, achieving the best-possible parallel runtime requires $2|N| + 2|E|$ cores working in parallel.

V. Experimental Evaluation

This section assesses the benefits of all three SDP strengthening approaches in a step-wise fashion. The assessment is done by comparing four variants of the SDP relaxation for bounding primal AC-OPF solutions produced by IPOPT, which only guarantees local optimality. The four relaxations under consideration are as follows:

1) SDP-N : the SDP relaxation strengthened with the bound tightening proposed in [19].
2) SDP-N+LNC : SDP-N with the addition of lifted nonlinear cuts.
3) SDP-N+QC : SDP-N with the conjunction of the QC model.
4) SDP-N+QC+LNC : SDP-N with the conjunction of the QC model and lifted nonlinear cuts.

Experimental Setting: All of the computations are performed on Dell PowerEdge R415 servers with Dual 3.1GHz AMD 6-Core Opteron 4334 CPUs and 64GB of memory. IPOPT 3.12 [48] with linear solver ma27 [49], is used as a heuristic for finding locally optimal feasible solutions to the non-convex AC-OPF problem formulated in AMPL, [50]. The SDP models were solved using SDPT3 4.0 [51] with the modifications suggested in [52]. The SDP relaxations utilize the sparsity exploiting implementation [52], which benefits from performance and scalability gains due to a branch decomposition scheme [20]. The tight variable bounds for SDP-N are pre-computed using the algorithm in [19]. If all of the subproblems are computed in parallel, the bound tightening computation adds an overhead of less than 1 minute, which is not reflected in the runtime results presented here.

Open Test Cases: NESTA v0.6.0 [16] contains 115 test cases ranging from 3 to 9000 buses. The cases are broken into five categories; a typical operating condition (TYP); congested operating condition (API); a small angle difference condition (SAD); non-convex optimization tests (NCO) from [46]; and radial network tests (RAD) from [17]. The TYP, API, and SAD categories are design to be realistic operating conditions, while the NCO and RAD categories are less realistic, but useful for testing optimization methods.

Due to the computational burden of using modern SDP solvers on cases with more than 1000-buses [18], [7] and our lack of a large-scale distributed implementation of Algorithm 1, the evaluation was conducted on the 71 test cases that have less than 1000-buses. Among these 71 test cases, it is observed that combining the SDP with the bound propagation (i.e., SDP-N) was sufficient to close the optimality gap to less than 1.0% on 55 cases (see the Appendix for detailed results), leaving 16 open test cases Hence, we focus our attention on those test cases where the SDP-N optimality gap is greater than 1.0%. Detailed performance and runtime results are present in Table I and can be summarized as follows:

1) SDP-N+LNC brings significant improvements to the SDP-N relaxation, most often reducing the optimality gap by several percentage points.
2) SDP-N+QC is generally stronger than SDP-N+LNC with the exception of case162_ieee_dtc__sad, case9_na_cao__nco and case9_nb_cao__nco, illustrating that there is value in adding both the QC model and the lifted nonlinear cuts to the SDP relaxation.
3) The strongest model, SDP-N+QC+LNC, reduceds the optimality gap of 8 of the 16 of the open cases to less

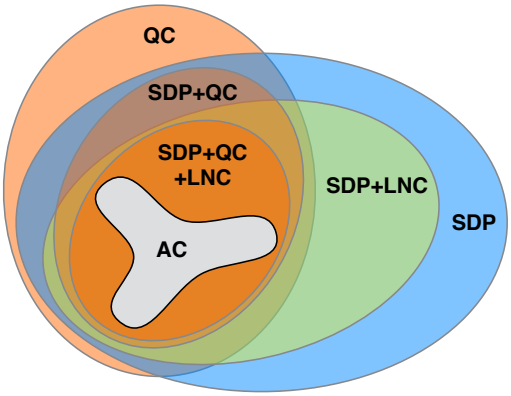

Fig. 2: A Venn Diagram of the Solutions Sets for Various SDP Relaxations (set sizes in this illustration are not to scale).

than 1% (i.e., closing 50% of the open cases), leaving only 8 for further investigation. Furthermore, on 5 of the 8 open cases, the AC solution is known to be globally optimal, indicating that the only source of the optimality gap comes from convexificaiton. These cases are ideal candidates for evaluation of non-convex optimization algorithms.

4) Although the SDP-N+QC model requires substantially more constraints than SDP-N+LNC, the runtimes do not vary significantly. We suspect that the SDP iteration computation dominates the runtime on these test cases.

Relations between the Power Flow Relaxations: From the results presented in Table I, we can conclude that combining SDP-N with the QC model, and adding the LNCs leads to a relaxation that strictly dominates all others. Using this information, Figure 2 presents an updated Venn Diagram of relaxations (originally presented in [18]) to reflect the various strengthened relaxations considered here.

VI. Conclusion

With several years of steady progress on convex relaxations of the AC power flow equations, the optimality gap on the vast majority of AC Optimal Power Flow (AC-OPF) test cases has been closed to less than 1%. This work sought to push the limits of convex relaxations even further and close the optimality gap on the 16 remaining open test cases. To that end, the SDP-N+QC+LNC power flow relaxation was developed by hybridizing the SDP and QC relaxations, integrating the LNCs valid inequalities, and performing bound propagation. The proposed model was able to reduce the optimality gap to less than 1% on 8 of the 16 open cases. Overall, SDP-N+QC+LNC is able to close the gap on 88.7% of the 71 AC-OPF cases considered herein.

The key weakness of the SDP-N+QC+LNC relaxation is its reliance on SDP solving technology, which suffers from scalability limitations [18], [7]. Fortunately, recent works have proposed promising approaches for scaling the SDP relaxations to larger test cases [53], [43]. Despite the current scalability challenges, it may still be beneficial to perform this costly SDP computation at the root node of a branch-and-bound algorithm to produce a tight lower bound. Indeed, after ten hours of computation, off-the-shelf global optimization solvers [54], [55] cannot close the optimality gap on the vast majority of AC-OPF test cases.

An interesting avenue for future work is to better understand the theoretical relationship between the methods developed in this paper to line of moment-based relaxations that have been developed in [6], [7], [8], [9]. These approaches begin with the SDP relaxation (i.e. Model 2) and add higher-order SDP constraints that tighten the relaxation further. The relationship between these higher-order constraints and the QC and LNC constraints with bound tightening has not yet been investigated. It would be ideal to understand the theoretical relationships between these higher moments in the context of Figure 2.

More broadly, this work highlights two notable facts about the classic AC-OPF problem. First, interior point methods (e.g., IPOPT) are able to find globally optimal solutions in the vast majority of test cases. Second, it is possible to enclose the non-convex AC-OPF feasibility region in a tight convex set, leading to relaxations with very small optimality gaps. Both of these results are interesting given that the AC-OPF is a non-convex optimization problem, which is known to be NP-Hard in general [23], [24].

Acknowledgements

NICTA is funded by the Australian Government through the Department of Communications and the Australian Research Council through the ICT Centre of Excellence Program.

References

[1] C. Coffrin, H. L. Hijazi, and P. V. Hentenryck, "Strengthening the SDP Relaxation of AC Power Flows with Convex Envelopes, Bound Tightening, and Lifted Nonlinear Cuts," *CoRR*, vol. abs/1512.04644, 2015. [Online]. Available: http://arxiv.org/abs/1512.04644

[2] R. Jabr, "Radial distribution load flow using conic programming," *IEEE Transactions on Power Systems*, vol. 21, no. 3, pp. 1458–1459, Aug 2006.

[3] M. Farivar, C. Clarke, S. Low, and K. Chandy, "Inverter var control for distribution systems with renewables," in *2011 IEEE International Conference on Smart Grid Communications (SmartGridComm)*, Oct 2011, pp. 457–462.

[4] H. Hijazi, C. Coffrin, and P. Van Hentenryck, "Convex quadratic relaxations of mixed-integer nonlinear programs in power systems," Published online at http://www.optimization-online.org/DB_HTML/2013/09/4057.html, 2013.

[5] X. Bai, H. Wei, K. Fujisawa, and Y. Wang, "Semidefinite programming for optimal power flow problems," *International Journal of Electrical Power & Energy Systems*, vol. 30, no. 6-7, pp. 383 – 392, 2008.

[6] D. Molzahn and I. Hiskens, "Moment-based relaxation of the optimal power flow problem," in *Power Systems Computation Conference (PSCC), 2014*, Aug 2014, pp. 1–7.

[7] B. Ghaddar, J. Marecek, and M. Mevissen, "Optimal power flow as a polynomial optimization problem," *IEEE Transactions on Power Systems*, vol. 31, no. 1, pp. 539–546, Jan 2016.

[8] D. K. Molzahn and I. A. Hiskens, "Sparsity-exploiting moment-based relaxations of the optimal power flow problem," *IEEE Transactions on Power Systems*, vol. 30, no. 6, pp. 3168–3180, Nov 2015.

[9] C. Josz and D. K. Molzahn, "Moment/Sum-of-Squares Hierarchy for Complex Polynomial Optimization," *CoRR*, vol. abs/1508.02068, 2015. [Online]. Available: http://arxiv.org/abs/1508.02068

[10] J. Lavaei and S. Low, "Zero duality gap in optimal power flow problem," *IEEE Transactions on Power Systems*, vol. 27, no. 1, pp. 92 –107, feb. 2012.

[11] R. Zimmerman, C. Murillo-Sandnchez, and R. Thomas, "Matpower: Steady-state operations, planning, and analysis tools for power systems research and education," *IEEE Transactions on Power Systems*, vol. 26, no. 1, pp. 12 –19, feb. 2011.

TABLE I: Quality and Runtime Results of AC Power Flow Relaxations (Open Cases).

	$/h	Optimality Gap (%)				Runtime (seconds)				
Test Case	AC	SDP-N	+LNC	+QC	+QC +LNC	AC	SDP-N	+LNC	+QC	+QC +LNC
Typical Operating Conditions (TYP)										
nesta_case5_pjm	**17551.89**	5.22	5.06	3.96	3.96	0.16	3.18	2.92	3.36	3.04
Congested Operating Conditions (API)										
nesta_case30_fsr__api	372.14	3.58	1.03	0.89	0.61	0.09	3.63	5.38	5.46	5.56
nesta_case89_pegase__api	4288.02	18.11	18.08⋆	17.09⋆	16.60⋆	0.50	12.44	13.17	47.50	28.27
nesta_case118_ieee__api	10325.27	16.72	8.70	3.40	3.32	0.40	8.49	9.61	10.73	13.62
Small Angle Difference Conditions (SAD)										
nesta_case24_ieee_rts__sad	79804.30	1.38	0.05	0.07	0.02	0.20	3.80	4.13	3.27	3.77
nesta_case29_edin__sad	46931.74	5.79	1.90	0.53	0.50	0.35	4.70	5.34	6.23	6.11
nesta_case73_ieee_rts__sad	235241.58	2.41	0.18	0.05	0.03	0.26	6.44	6.80	8.01	8.51
nesta_case118_ieee__sad	4324.17	4.04	1.16	0.83	0.74	0.32	11.21	10.44	11.65	14.31
nesta_case162_ieee_dtc__sad	4369.19	1.73	0.37	1.49	0.35	0.68	20.16	20.18	53.54	40.58
nesta_case189_edin__sad	914.64	1.20⋆	0.89⋆	err.⋆	0.86⋆	0.29	7.51	10.91	36.24	54.44
Non-Convex Optimization Cases (NCO)										
nesta_case9_na_cao__nco	**-212.43**	18.00	11.66	15.91	11.62	0.05	2.42	2.66	3.26	2.30
nesta_case9_nb_cao__nco	**-247.42**	19.23	11.77	16.46	11.76	0.18	2.44	2.55	2.06	2.31
nesta_case14_s_cao__nco	9670.44	2.96	2.92	2.06	2.03	0.07	3.21	2.86	2.91	3.10
Radial Topologies (RAD)										
nesta_case9_kds__rad	11279.48	1.09	0.13	1.04⋆	0.13	0.29	2.47	2.34	2.08	2.54
nesta_case30_kds__rad	**4336.18**†	2.11	1.88	1.97	1.88	n.a.	4.02	3.25	6.51	3.84
nesta_case30_l_kds__rad	**3607.73**†	15.86	15.56	15.76	15.56	n.a.	3.53	3.28	4.69	4.26

bold - known global optimum, † - best known solution (not initial IPOPT solution), ⋆ - solver reported numerical accuracy warnings.

[12] Gurobi Optimization, Inc., "Gurobi optimizer reference manual," Published online at http://www.gurobi.com, 2014.

[13] I. IBM, "IBM ILOG CPLEX Optimization Studio," http://www-01.ibm.com/software/commerce/optimization/cplex-optimizer/, 2014.

[14] MOSEK ApS, *The MOSEK optimization toolbox.*, 2015. [Online]. Available: http://www.mosek.com/resources/doc

[15] B. Lesieutre, D. Molzahn, A. Borden, and C. DeMarco, "Examining the limits of the application of semidefinite programming to power flow problems," in *49th Annual Allerton Conference on Communication, Control, and Computing (Allerton), 2011*, sept. 2011, pp. 1492 –1499.

[16] C. Coffrin, D. Gordon, and P. Scott, "NESTA, The NICTA Energy System Test Case Archive," *CoRR*, vol. abs/1411.0359, 2014. [Online]. Available: http://arxiv.org/abs/1411.0359

[17] B. Kocuk, S. Dey, and X. Sun, "Inexactness of SDP relaxation and valid inequalities for optimal power flow," *IEEE Transactions on Power Systems*, vol. PP, no. 99, pp. 1–10, 2015.

[18] C. Coffrin, H. Hijazi, and P. Van Hentenryck, "The QC Relaxation: A Theoretical and Computational Study on Optimal Power Flow," *IEEE Transactions on Power Systems*, pp. 1–11, (forthcoming) 2015.

[19] ——, "Strengthening convex relaxations with bound tightening for power network optimization," in *Principles and Practice of Constraint Programming*, ser. Lecture Notes in Computer Science, G. Pesant, Ed. Springer International Publishing, 2015, vol. 9255, pp. 39–57. [Online]. Available: http://dx.doi.org/10.1007/978-3-319-23219-5_4

[20] R. Madani, M. Ashraphijuo, and J. Lavaei, "Promises of conic relaxation for contingency-constrained optimal power flow problem," *IEEE Transactions on Power Systems*, 2015.

[21] J. Taylor and F. Hover, "Convex models of distribution system reconfiguration," *IEEE Transactions on Power Systems*, vol. 27, no. 3, pp. 1407–1413, Aug 2012.

[22] M. J. Carpentier, "Contribution a letude du dispatching economique," Bulletin Society Francaise Electriciens, Aug. 1962.

[23] A. Verma, "Power grid security analysis: An optimization approach," Ph.D. dissertation, Columbia University, 2009.

[24] K. Lehmann, A. Grastien, and P. Van Hentenryck, "AC-Feasibility on Tree Networks is NP-Hard," *IEEE Transactions on Power Systems*, 2015 (to appear).

[25] J. Momoh, R. Adapa, and M. El-Hawary, "A review of selected optimal power flow literature to 1993. i. nonlinear and quadratic programming approaches," *IEEE Transactions on Power Systems*, vol. 14, no. 1, pp. 96 –104, feb 1999.

[26] J. Momoh, M. El-Hawary, and R. Adapa, "A review of selected optimal power flow literature to 1993. ii. newton, linear programming and interior point methods," *IEEE Transactions on Power Systems*, vol. 14, no. 1, pp. 105 –111, feb 1999.

[27] C. Coffrin, H. Hijazi, and P. Van Hentenryck, "Network Flow and Copper Plate Relaxations for AC Transmission Systems," *CoRR*, vol. abs/1506.05202, 2015. [Online]. Available: http://arxiv.org/abs/1506.05202

[28] F. Capitanescu, J. M. Ramos, P. Panciatici, D. Kirschen, A. M. Marcolini, L. Platbrood, and L. Wehenkel, "State-of-the-art, challenges, and future trends in security constrained optimal power flow," *Electric Power Systems Research*, vol. 81, no. 8, pp. 1731 – 1741, 2011. [Online]. Available: http://www.sciencedirect.com/science/article/pii/S0378779611000885

[29] B. Stott and O. Alsac, "Optimal power flow — basic requirements for real-life problems and their solutions," self published, available from brianstott@ieee.org, Jul 2012.

[30] C. Coffrin, H. Hijazi, K. Lehmann, and P. Van Hentenryck, "Primal and dual bounds for optimal transmission switching," *Power Systems Computation Conference (PSCC)*, pp. 1–8, 08 2014.

[31] C. Coffrin, H. Hijazi, and P. Van Hentenryck, "DistFlow Extensions for AC Transmission Systems," *CoRR*, vol. abs/1506.04773, 2015. [Online]. Available: http://arxiv.org/abs/1506.04773

[32] B. Subhonmesh, S. Low, and K. Chandy, "Equivalence of branch flow and bus injection models," in *Communication, Control, and Computing (Allerton), 2012 50th Annual Allerton Conference on*, Oct 2012, pp. 1893–1899.

[33] S. Sojoudi and J. Lavaei, "Physics of power networks makes hard optimization problems easy to solve," in *Power and Energy Society General Meeting, 2012 IEEE*, July 2012, pp. 1–8.

[34] L. Vandenberghe and S. Boyd, "Semidefinite programming," *SIAM Review*, vol. 38, no. 1, pp. 49–95, 1996. [Online]. Available: http://dx.doi.org/10.1137/1038003

[35] R. M. Freund, "Introduction to Semidefinite Programming (SDP)," Published online at http://ocw.mit.edu/courses/electrical-engineering-and-computer-science/6-251j-introduction-to-mathematical-programming-fall-2009/readings/MIT6_251JF09_SDP.pdf, Sept. 2009.

[36] A. Gomez Esposito and E. Ramos, "Reliable load flow technique for radial distribution networks," *IEEE Transactions on Power Systems*, vol. 14, no. 3, pp. 1063–1069, Aug 1999.

[37] R. Jabr, "Optimal power flow using an extended conic quadratic formulation," *IEEE Transactions on Power Systems*, vol. 23, no. 3, pp. 1000–1008, Aug 2008.

[38] F. Capitanescu, I. Bilibin, and E. Romero Ramos, "A comprehensive centralized approach for voltage constraints management in active distribution grid," *IEEE Transactions on Power Systems*, vol. 29, no. 2, pp. 933–942, March 2014.

[39] E. Romero-Ramos, J. Riquelme-Santos, and J. Reyes, "A simpler and exact mathematical model for the computation of the minimal power losses tree," *Electric Power Systems Research*, vol. 80, no. 5, pp. 562 – 571, 2010. [Online]. Available: http://www.sciencedirect.com/science/article/pii/S0378779609002570
[40] G. McCormick, "Computability of global solutions to factorable nonconvex programs: Part i - convex underestimating problems," *Mathematical Programming*, vol. 10, pp. 146–175, 1976.
[41] L. Liberti, "Reduction constraints for the global optimization of nlps," *International Transactions in Operational Research*, vol. 11, no. 1, pp. 33–41, 2004. [Online]. Available: http://dx.doi.org/10.1111/j.1475-3995.2004.00438.x
[42] J. P. Ruiz and I. E. Grossmann, "Using redundancy to strengthen the relaxation for the global optimization of MINLP problems," *Computers & Chemical Engineering*, vol. 35, no. 12, pp. 2729 – 2740, 2011.
[43] B. Kocuk, S. S. Dey, and X. A. Sun, "Strong SOCP Relaxations for the Optimal Power Flow Problem," *CoRR*, vol. abs/1504.06770, 2015. [Online]. Available: http://arxiv.org/abs/1504.06770
[44] C. Chen, A. Atamturk, and S. Oren, "Bound tightening for the alternating current optimal power flow problem," *IEEE Transactions on Power Systems*, vol. PP, no. 99, pp. 1–8, 2015.
[45] J. E. Prussing, "The principal minor test for semidefinite matrices," *Journal of Guidance, Control, and Dynamics*, vol. 9, no. 1, pp. 121–122, 2015/09/28 1986.
[46] C. Chen, A. Atamturk, and S. S. Oren, "A spatial branch-and-cut algorithm for nonconvex QCQP with bounded complex variables," Published online at http://ieor.berkeley.edu/~atamturk/pubs/sbc.pdf, Aug. 2015.
[47] R. Madani, S. Sojoudi, and J. Lavaei, "Convex relaxation for optimal power flow problem: Mesh networks," *IEEE Transactions on Power Systems*, vol. 30, no. 1, pp. 199–211, Jan 2015.
[48] A. Wächter and L. T. Biegler, "On the implementation of a primal-dual interior point filter line search algorithm for large-scale nonlinear programming," *Mathematical Programming*, vol. 106, no. 1, pp. 25–57, 2006.
[49] R. C. U.K., "The hsl mathematical software library," Published online at http://www.hsl.rl.ac.uk/, accessed: 30/10/2014.
[50] R. Fourer, D. M. Gay, and B. Kernighan, "AMPL: A Mathematical Programming Language," in *Algorithms and Model Formulations in Mathematical Programming*, S. W. Wallace, Ed. New York, NY, USA: Springer-Verlag New York, Inc., 1989, pp. 150–151.
[51] K. C. Toh, M. Todd, and R. H. Tutuncu, "Sdpt3 – a matlab software package for semidefinite programming," *Optimization Methods and Software*, vol. 11, pp. 545–581, 1999.
[52] J. Lavaei, "OPF solver," Published online at http://www.ee.columbia.edu/~lavaei/Software.html, oct. 2014, accessed: 22/02/2015.
[53] H. Hijazi, C. Coffrin, and P. Van Hentenryck, "Polynomial SDP Cuts for Optimal Power Flow," *CoRR*, vol. abs/1510.08107, 2015. [Online]. Available: http://arxiv.org/abs/1510.08107
[54] T. Achterberg, "SCIP: solving constraint integer programs," *Mathematical Programming Computation*, vol. 1, no. 1, pp. 1–41, 2009. [Online]. Available: http://dx.doi.org/10.1007/s12532-008-0001-1
[55] P. Belotti, "Couenne: User manual," Published online at https://projects.coin-or.org/Couenne/, 2009, accessed: 10/04/2015.

APPENDIX

This appendix presents the baseline results of the SDP relaxation on the NESTA v0.6.0 test cases. The SDP relaxations utilize the sparsity exploiting implementation [52], which benefits from performance and scalability gains due to a branch decomposition scheme [20]. This SDP formulation is then strengthened with the bound tightening proposed in [19] to produce SDP-N. SDP-N is considered the baseline for comparison in this paper and represents the best-known results on the NESTA v0.6.0 test cases at this time.

Table II and Table III present the results. The base SDP relaxation is quite strong and closes the optimality gap to $< 1\%$ on 45 of the 71 cases. In the remaining 26 cases, the bound tightening procedure from [19] (i.e. SDP-N) decreases the gaps significantly and reduces 10 more cases below a gap of $< 1\%$. The remaining 16 cases with a significant optimally gap are the subject of this work.

TABLE II: Baseline Quality and Runtime Results of AC Power Flow Relaxations (All Cases).

Test Case	$/h AC	Opt. Gap (%) SDP	Opt. Gap (%) SDP-N	Runtime (seconds) AC	Runtime (seconds) SDP	Runtime (seconds) SDP-N
Typical Operating Conditions (TYP)						
nesta_case3_lmbd	5812.64	0.39	0.14	0.04	2.47	2.43
nesta_case4_gs	156.43	**0.00**	**0.00**	0.07	2.69	2.49
nesta_case5_pjm	17551.89	5.22	5.22	0.04	3.90	3.18
nesta_case6_c	23.21	0.00	0.00	0.04	3.04	3.13
nesta_case6_ww	3143.97	**0.00**	**0.00**	0.04	3.63	3.20
nesta_case9_wscc	5296.69	0.00	0.00	0.04	2.59	2.61
nesta_case14_ieee	244.05	**0.00**	**0.00**	0.07	3.13	2.57
nesta_case24_ieee_rts	63352.20	**0.00**	**0.00**	0.08	3.74	3.59
nesta_case29_edin	29895.49	**0.00**	**0.00**	0.34	5.29	4.99
nesta_case30_as	803.13	0.00	0.00	0.06	5.65	3.58
nesta_case30_fsr	575.77	0.00	0.00	0.06	5.17	3.86
nesta_case30_ieee	204.97	**0.00**	**0.00**	0.07	3.57	3.28
nesta_case39_epri	96505.52	0.01	0.01	0.07	3.88	4.29
nesta_case57_ieee	1143.27	**0.00**	**0.00**	0.12	4.86	5.40
nesta_case73_ieee_rts	189764.08	**0.00**	**0.00**	0.18	4.96	5.32
nesta_case89_pegase	5819.81	0.00	0.00	0.19	13.32	11.89
nesta_case118_ieee	3718.64	0.06	0.06	0.27	7.84	8.25
nesta_case162_ieee_dtc	4230.23	1.08	0.92	0.35	24.96	22.11
nesta_case189_edin	849.29	0.07	0.07	0.27	7.18	8.58
nesta_case300_ieee	16891.28	0.08	0.07	0.60	15.50	14.09
Congested Operating Conditions (API)						
nesta_case3_lmbd__api	367.74	1.26	0.00	0.05	2.45	3.16
nesta_case4_gs__api	767.27	**0.00**	**0.00**	0.04	2.89	3.191
nesta_case5_pjm__api	2998.54	**0.00**	**0.00**	0.04	3.96	3.56
nesta_case6_c__api	814.41	**0.00**	**0.00**	0.04	3.49	3.11
nesta_case6_ww__api	273.76	0.00*	err.	0.24	34.58	3.36†
nesta_case9_wscc__api	656.60	**0.00**	**0.00**	0.05	2.33	2.52
nesta_case14_ieee__api	325.56	**0.00**	**0.00**	0.05	2.45	2.59
nesta_case24_ieee_rts__api	6421.37	1.45	0.72	0.09	4.31	3.96
nesta_case29_edin__api	295782.61	—	—	0.20	5.76†	5.08†
nesta_case30_as__api	571.13	0.00	0.00	0.07	4.16	4.23
nesta_case30_fsr__api	372.14	11.06	3.58	0.08	4.00	3.63
nesta_case30_ieee__api	415.53	0.00	0.00	0.07	4.29	4.14
nesta_case39_epri__api	7466.25	**0.00**	**0.00**	0.09	4.17	3.62
nesta_case57_ieee__api	1430.65	0.08	0.03	0.11	5.02	5.34
nesta_case73_ieee_rts__api	20123.98	4.29	0.86	0.35	6.21	7.07
nesta_case89_pegase__api	4288.02	18.11	18.11	0.67	13.27	12.44
nesta_case118_ieee__api	10325.27	31.50	16.72	0.36	7.46	8.49
nesta_case162_ieee_dtc__api	6111.68	0.85	0.54	1.51	28.12	31.67
nesta_case189_edin__api	1982.82	0.05*	0.05	0.72	14.50	8.60
nesta_case300_ieee__api	22866.03	0.00	0.00	0.60	15.97	17.31

bold - relaxation recovered a feasible solution, † - solver failed to converge,
$\star$ - solver reported numerical accuracy warnings.

TABLE III: Baseline Quality and Runtime Results of AC Power Flow Relaxations (All Cases, Cont.).

Test Case	$/h AC	Opt. Gap (%) SDP	Opt. Gap (%) SDP-N	Runtime (seconds) AC	Runtime (seconds) SDP	Runtime (seconds) SDP-N
Small Angle Difference Conditions (SAD)						
nesta_case3_lmbd__sad	5992.72	2.06	0.09	0.04	2.38	2.33
nesta_case4_gs__sad	324.02	0.05	0.00	0.04	2.74	2.80
nesta_case5_pjm__sad	26423.19	**0.00**	**0.00**	0.04	3.55	3.33
nesta_case6_c__sad	24.43	0.00	0.00	0.04	3.30	2.88
nesta_case6_ww__sad	3149.51	**0.00**	**0.00**	0.05	3.52	3.55
nesta_case9_wscc__sad	5590.11	0.00	0.00	0.04	2.54	2.81
nesta_case14_ieee__sad	244.15	0.00	0.00	0.05	2.75	2.70
nesta_case24_ieee_rts__sad	79804.30	6.05	1.38	0.08	3.49	3.80
nesta_case29_edin__sad	46931.74	28.44	5.79	0.37	5.28	4.70
nesta_case30_as__sad	914.44	0.47	0.12	0.07	3.13	3.68
nesta_case30_fsr__sad	577.73	0.07	0.07	0.06	3.35	3.48
nesta_case30_ieee__sad	205.11	**0.00**	**0.00**	0.08	3.60	4.17
nesta_case39_epri__sad	97219.01	0.09	0.04	0.08	3.87	3.52
nesta_case57_ieee__sad	1143.89	0.02	0.00	0.10	4.59	4.26
nesta_case73_ieee_rts__sad	235241.58	4.10	2.41	0.25	4.97	6.44
nesta_case89_pegase__sad	5827.01	0.03	0.03	0.19	29.63	25.83
nesta_case118_ieee__sad	4324.17	7.57	4.04	0.35	8.48	11.21
nesta_case162_ieee_dtc__sad	4369.19	3.65	1.73	0.60	29.03	20.16
nesta_case189_edin__sad	914.64	1.21⋆	1.20⋆	0.31	8.22	7.51
nesta_case300_ieee__sad	16910.23	0.13	0.11	0.62	15.11	14.45
Non-Convex Optimization Cases (NCO)						
nesta_case9_na_cao__nco	-212.43	18.00	18.00	0.04	2.87	2.42
nesta_case9_nb_cao__nco	-247.42	19.29	19.23	0.04	2.76	2.44
nesta_case14_s_cao__nco	9670.44	2.97	2.96	0.05	3.05	3.21
Radial Topologies (RAD)						
nesta_case9_kds__rad	11279.48	52.70	1.09	0.07	2.35	2.47
nesta_case9_l_kds__rad	1756.52	15.63	0.40	0.07	2.35	2.22
nesta_case30_fsr_kds__rad	619.04	1.73	0.00	0.08	3.19	3.66
nesta_case30_fsr_l_kds__rad	445.84	2.25	0.00	0.07	3.27	3.93
nesta_case30_kds__rad	4794.31	11.47	11.47	0.06	4.03	4.02
nesta_case30_l_kds__rad	4562.25	33.46	33.46	0.07	3.24	3.53
nesta_case57_kds__rad	12100.84	13.58	0.02	0.07	3.80	3.80
nesta_case57_l_kds__rad	10172.97	17.43	0.02	0.08	4.91	4.17

bold - relaxation recovered a feasible solution, † - solver failed to converge,
⋆ - solver reported numerical accuracy warnings.